

REMARKS

Two photographs, original Figures 16A and 16B and 32 from parent application 08/192,093, filed February 4, 1994, have been deleted. The original photographs were unavailable and unnecessary for an understanding of the invention. Amendments to the Specification have been made to correct inadvertent typographical errors and informalities and to renumber the Figures in the Specification to correspond with the drawings filed on July 5, 2002. Support for these amendments is found in the figures and corresponding paragraphs as originally filed. Claims 23, 48 and 49 have been cancelled. The title has been amended to be more descriptive of the claimed invention. Support for this amendment is found in the specification at page 61, lines 15-27. No new matter has been added.

Preliminary Amendment

A Preliminary Amendment was filed on July 5, 2002. Entry of the Preliminary Amendment is respectfully requested.

Information Disclosure Statement

An Information Disclosure Statement was filed on September 13, 2002. Entry of the Information Disclosure Statement is respectfully requested.

09/897,724

-23-

CONCLUSION

In view of the above amendments and remarks, it is believed that all claims are in condition for allowance, and it is respectfully requested that the application be passed to issue. If the Examiner feels that a telephone conference would expedite prosecution of this case, the Examiner is invited to call the undersigned at (978) 341-0036.

Respectfully submitted,

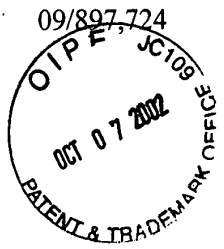
HAMILTON, BROOK, SMITH & REYNOLDS, P.C.

By Deirdre E. Sanders

Deirdre E. Sanders  
Registration No. 42,122  
Telephone: (978) 341-0036  
Facsimile: (978) 341-0136

Concord, MA 01742-9133

Dated: October 3, 2002



-i-

MARKED UP VERSION OF AMENDMENTS

Specification Amendments Under 37 C.F.R. § 1.121(b)(1)(iii)

Replace the title at page 1, lines 1 through 2 with the following title marked up by way of bracketing and underlining to show the changes relative to the previous version of the title.

METHODS OF TREATING BLOOD PATHOLOGY WITH CHIMERIC ANTI-TNF  
ANTIBODIES [AND PEPTIDES OF HUMAN TUMOR NECROSIS FACTOR]

Replace the paragraph at page 12, lines 19 through 24 with the below paragraph marked up by way of bracketing and underlining to show the changes relative to the previous version of the paragraph.

[Figure 17A-17B] Figures 16A-16B. Figure 16A [17A] is a nucleic acid sequence (SEQ ID NO:2) and corresponding amino acid sequence (SEQ ID NO:3) of a cloned cA2 light chain variable region. Figure 16B [17B] is a nucleic acid sequence (SEQ ID NO:4) and corresponding amino acid sequence (SEQ ID NO:5) of a cloned cA2 heavy chain variable region [constant region (SEQ ID NO:3)].

Replace the paragraph at page 12, lines 25 through 30 with the below paragraph marked up by way of bracketing and underlining to show the changes relative to the previous version of the paragraph.

Figure 17 [18] is a graphical representation of the early morning stiffness for the five patients in group I, and the four patients in group II is plotted as the mean percent of the baseline value versus time. Both groups showed an approximately 80 percent decrease or greater in early morning stiffness, which persisted for greater than 40 days.

Replace the paragraph at page 12, lines 31 through 37 with the below paragraph marked up by way of bracketing and underlining to show the changes relative to the previous version of the paragraph.

Figure 18 [19] is a graphical representation of the assessment of pain using a visual analogue scale for the five patients in group I, and the four patients in group II, is plotted as the mean percent of the baseline value versus time. Both groups showed an approximately 60 to 80 percent decrease in pain score which persisted for greater than 40 days.

Replace the paragraph at page 13, lines 1 through 6 with the below paragraph marked up by way of bracketing and underlining to show the changes relative to the previous version of the paragraph.

Figure 19 [20] is a graphical representation of the Ritchie Articular Index, (a scale scored of joint tenderness), is plotted as the mean percent of the baseline value versus time. Both groups showed an approximately 80 percent decrease in the Ritchie Articular Index, which persisted for greater than 40 days.

Replace the paragraph at page 13, lines 7 through 12 with the below paragraph marked up by way of bracketing and underlining to show the changes relative to the previous version of the paragraph.

Figure 20 [21] is a graphical representation of the number of swollen joints for the five patients in group I and the four patients in Group II is plotted as the mean percent of baseline value versus time. Both groups showed an approximately 70 to 80 percent decrease in swollen joints, which persisted for 30 to 40 days.

Replace the paragraph at page 13, lines 13 through 21 with the below paragraph marked up by way of bracketing and underlining to show the changes relative to the previous version of the paragraph.

Figure 21 [22] is a graphical representation of the serum C-reactive protein for four to five patients in group I, and three of the [for] four patients in group II, is plotted as the mean percent of the baseline value versus time. Both groups showed an approximately 80 percent reduction in CRP which persisted for 30 to 40 days. The values for patient number 1 and patient number 7 were omitted from the computations on which the plots are based, since these patients did not have elevated CRP values at baseline.

Replace the paragraph at page 13, lines 22 through 30 with the below paragraph marked up by way of bracketing and underlining to show the changes relative to the previous version of the paragraph.

Figure 22 [23] is a graphical representation of the erythrocyte sedimentation rate for the five patients in group I and three of the patients in group II is plotted as the mean percent of the baseline value versus time. Both groups showed an approximately 40 percent reduction in ESR which persisted for at least 40 days. The data from patient number 9 is omitted from the computations on which the plots were based, since this patient did not have an elevated ESR at baseline.

Replace the paragraph at page 13, lines 31 through 37 with the below paragraph marked up by way of bracketing and underlining to show the changes relative to the previous version of the paragraph.

Figure 23 [24] is a graphical representation of the index of Disease Activity, (a composite score of several parameters of disease activity), for the five patients in group I, and the four patients in group II, is plotted as the mean percent of the baseline value versus time. Both groups showed a clinically significant reduction in IDA, which persisted for at least 40 days.

Replace the paragraph at page 14, lines 1 through 9 with the below paragraph marked up by way of bracketing and underlining to show the changes relative to the previous version of the paragraph.

Figure 24 [25] is a graphical representation of swollen joint counts (maximum 28), as recorded by a single observer. Circles represent individual patients and horizontal bars show median values at each time point. The screening time point was within 4 weeks of entry to the study (week 0); data from patient 15 were not included after week 2 (dropout). Significance of the changes, relative to week 0, by Mann-Whitney test, adjusted: week 1,  $p>0.05$ ; week 2,  $p<0.02$ ; weeks 3-4,  $p<0.002$ ; weeks 6-8,  $p<0.001$ .

Replace the paragraph at page 14, lines 10 through 21 with the below paragraph marked up by way of bracketing and underlining to show the changes relative to the previous version of the paragraph.

Figure 25 [26] is a graphical representation of levels of serum C - reactive protein (CRP) - Serum CRP (normal range 0-10 mg/liter), measured by nephelometry. Circles represent individual patients and horizontal bars show median values at each time point. The screening time point was within 4 weeks of entry to the study (week 0); data from patient 15 were not included after week 2 (dropout). Significance of the changes, relative to week 0, by Mann-Whitney test, adjusted: week 1,  $p<0.001$ ; week 2,  $p<0.003$ ; week 3,  $p<0.002$ ; week 4,  $p<0.02$ ; week 6,8,  $p<0.001$ . Figure 28 [27B] is a schematic illustration of the construction of the vectors used to express the heavy chain of the immunoreceptors.

Replace the paragraph at page 14, line 22 through page 15, line 14 with the below paragraph marked up by way of bracketing and underlining to show the changes relative to the previous version of the paragraph.

[Figure 27A-27B] Figures 26A-26B. Figure 26A [27A] is a schematic [aschematic] illustration of the genes encoding TNF receptor/IgG fusion proteins and the gene encoding the truncated light chain. The gene encoding Ig heavy chain (IgH) fusion proteins had the same basic structure as the naturally occurring, rearranged Ig genes except that the Ig variable region coding sequence was replaced with TNF receptor coding sequence. Except for the TNF receptor coding

sequences and a partial human K sequence derived by modifying the murine J region coding sequence in the cM-T412 IgH gene by PCT mutagenesis, the entire genomic fragment shown originated from the cM-T412 chimeric mouse/human IgH gene. Looney et al., *Hum. Antibody Hybrid.* 3:191-200 (1992). The region deleted in the genes encoding p55-sf3 and p75P-sf3 is marked in the figure. The JC<sub>K</sub> gene, encoding a truncated Ig Kappa light chain, was constructed by deleting the variable region coding sequence from the cM-T412 chimeric mouse/human Ig Kappa gene (Looney, *infra*) and using PCR mutagenesis to change the murine J sequence to a partial human J sequence. The p55-light chain fusion in p55-df2 was made by inserting the p55 coding sequence into the EcoRV site in the JC<sub>K</sub> gene. Tracey et al., *Nature* 330:662-666 (1987). Figure 26B [27B] is a schematic illustration of several immunoreceptor molecules of the present invention. The blackened ovals each represent a domain of the IgGl constant region. The [THe] circles represent the truncated light chain. Small circles adjacent to a p55 or p75 subunit mark the positions of human J sequence. The incomplete circles in p75-sf2 and -sf3 are to illustrate that the C-terminal 53 amino acids of the p75 extracellular domain were deleted. Lines between subunits represent disulfide bonds.

Replace the paragraph at page 15, lines 15 through 18 with the below paragraph marked up by way of bracketing and underlining to show the changes relative to the previous version of the paragraph.

Figure 27 [28] is a schematic illustration of the construction of a cM-T412 heavy [light] chain so that it has a unique cloning site for insertion of foreign genes such as p55 and p75.

Replace the paragraph at page 15, lines 19 through 21 with the below paragraph marked up by way of bracketing and underlining to show the changes relative to the previous version of the paragraph.

Figure 28 [29] is a schematic illustration of the construction of the vectors used to express the heavy [light] chain of the immunoreceptors.

Replace the paragraph at page 15, lines 22 through 25 with the below paragraph marked up by way of bracketing and underlining to show the changes relative to the previous version of the paragraph.

Figure 29 [30] is a schematic illustration of the construction of a cM-T412 light chain so that it has a unique cloning site for insertion of foreign genes such as p55 and p75.

Replace the paragraph at page 15, lines 26 through 28 with the below paragraph marked up by way of bracketing and underlining to show the changes relative to the previous version of the paragraph.

Figure 30 [31] is a schematic illustration of the construction of the vectors used to express the light chain of the immunoreceptors.

Replace the paragraph at page 16, lines 1 through 8 with the below paragraph marked up by way of bracketing and underlining to show the changes relative to the previous version of the paragraph.

[Figure 33A-C] Figures 31A-31C show [shows] graphical representations of fusion protein [proteins] protected WEHI 164 cells from TNF $\beta$  with actinomycin D and then incubated in 2 ng/ml TNF $\alpha$  with varying concentrations of TNF $\beta$  overnight at 37°C. Cell viability was determined by measuring their uptake of MTT dye. Figure 31A [33A] shows p55 fusion proteins. Figure 31B [33B] shows p75 fusion proteins. Figure 31C [33C] shows a comparison of the protective ability of the non-fusion form of p55 (p55-nf) to p55-sf2.

Replace the paragraph at page 16, lines 9 through 11 with the below paragraph marked up by way of bracketing and underlining to show the changes relative to the previous version of the paragraph.

Figure 32 [34] is a graphical representation [represation] of data showing fusion proteins also effectively protect WEHI 164 cells from TNF $\beta$  cytotoxicity.

Replace the paragraph at page 16, lines 12 through 27 with the below paragraph marked up by way of bracketing and underlining to show the changes relative to the previous version of the paragraph.

[Figure 35A-35B] Figures 33A-33H are [is a] graphical representations [representation] of analyses of binding between the various fusion proteins and TNF $\alpha$  by saturation binding (Figures 33A and 33B [Figure 35A]) and Scatchard analysis (Figures 33C-33H [Figure 35B]). A microtiter plate was coated with excess goat anti-Fc polyclonal antibody and incubated with 10 ng/ml of fusion protein in TBST buffer (10 mM Tris-HCl [HCl], pH 7.8, 150 mM NaCl [NaCl], 0.05% Tween-20) for 1 hour. Varying amounts of  $^{125}$ I labeled TNF $\alpha$  (specific activity - 34.8  $\mu$ Ci/ $\mu$ g) was then incubated with the captured fusion protein in PBS (10 mM Na Phosphate, pH 7.0, 150 mM NaCl) with 1% bovine serum albumin for 2 hours. Unbound TNF $\alpha$  was washed away with four washes in PBS and the cpm bound was quantitated using a y-counter. All samples were analyzed in triplicate. The slope of the lines in (Figures 33C-33H [Figure 35B]) represent the affinity constant,  $K_a$ . The dissociation constant ( $K_d$ ) values (see Table I) were derived using the equation  $K_d = I/K_a$ .

Replace the paragraph at page 20, lines 1 through 14 with the below paragraph marked up by way of bracketing and underlining to show the changes relative to the previous version of the paragraph.

Preferred antibodies of the present invention are high affinity human-murine chimeric anti-TNF antibodies, and fragments or regions thereof, that have potent inhibiting and/or neutralizing activity *in vivo* against human TNF $\alpha$ . Such antibodies and chimeric antibodies can include those generated by immunization using purified recombinant hTNF $\alpha$  (SEQ ID NO:1) or peptide fragments thereof. Such fragments can include epitopes of at least 5 amino acids of residues 87-108 [87-107], or a combination of both of 59-80 and 87-108 of hTNF $\alpha$  (as these corresponding amino acids of SEQ ID NO:1). Additionally, preferred antibodies, fragments and regions of anti-TNF antibodies of the present invention do not recognize amino acids from at least one of amino acids 11-13, 37-42, 49-57 or 155-157 of hTNF $\alpha$  (of SEQ ID NO:1).

Replace the paragraph at page 29, lines 1 through 12 with the below paragraph marked up by way of bracketing and underlining to show the changes relative to the previous version of the paragraph.

For example, a cDNA encoding a murine V region antigen-binding segment having anti-TNF activity can be provided using known methods based on the use of the DNA sequence presented in Figure 16A [17A] (SEQ ID NO:2). Alternatively, a cDNA encoding a murine C region antigen-binding segment having anti-TNF activity can be provided using known methods based on the use of the DNA sequence presented in Figure 16B [17B] (SEQ ID NO:3). Probes that bind a portion of the DNA sequence presented in Figure 16A [17A] or 16B [17B] can be used to isolate DNA from hybridomas expressing TNF antibodies, fragments or regions, as presented herein, according to the present invention, by known methods.

Replace the paragraph at page 29, lines 13 through 22 with the below paragraph marked up by way of bracketing and underlining to show the changes relative to the previous version of the paragraph.

Oligonucleotides representing a portion of the variable region presented in Figure 16A [17A] or 16B [17B] sequence are useful for screening for the presence of homologous genes and for the cloning of such genes encoding variable or constant regions of an anti-TNF antibody. Such probes preferably bind to portions of sequences according to Figures 16A [17A] or 16B [17B] which encode light chain or heavy chain variable regions which bind an activity inhibiting epitope of TNF, especially an epitope of at least 5 amino acids of residues 87-108 or a combination of residues 59-80 and 87-108 (of SEQ ID NO:1).

Replace the paragraph at page 40, lines 5 through 25 with the below paragraph marked up by way of bracketing and underlining to show the changes relative to the previous version of the paragraph.

In certain preferred embodiments, each of the two heavy chains and each of the two light chains is linked to a portion of the TNF receptor, thus forming a tetravalent molecule. Such a tetravalent molecule can have, for example, four p55 receptor molecules; two on the two heavy chains and two on the two light chains. Alternatively, a tetravalent molecule can have, for example, a p55 receptor molecule attached to each of the two heavy chains and a p75 receptor molecule attached to each of the two light chains. A tetravalent molecule can also have, for example, p55 receptor attached to the light chains and p75 receptor attached to the heavy chains. Additionally, a tetravalent molecule can have one heavy chain attached to p55, one heavy chain attached to p75, one light chain attached to p75, and one light chain attached to p55. See, for example, the molecules depicted in Figure 26A [27A]. Further, the molecules can have six receptors attached, for example; two within the heavy chains and four at the ends of the heavy and light chains. Other potential multimers and combinations would also be within the scope of one skilled in the art, once armed with the present disclosure.

Replace the paragraph at page 56, line 19 through page 57, line 16 with the below paragraph marked up by way of bracketing and underlining to show the changes relative to the previous version of the paragraph.

**Screening Methods** for determining tissue necrosis factor neutralizing and/or inhibiting activity are also provided in the present invention. In the context of the present invention, TNF neutralizing activity or TNF inhibiting activity refers to the ability of a TNF neutralizing compound to block at least one biological activity of TNF, such as preventing TNF from binding to a TNF receptor, blocking production of TNF by intracellular processing, such as transcription, translation or post-translational modification, expression on the cell surface, secretion or assembly of the bioactive trimer of TNF. Additionally, TNF neutralizing compounds can act by inducing regulation of metabolic pathways such as those involving the up or down regulation of TNF production. Alternatively TNF neutralizing compounds can modulate cellular sensitivity to TNF by decreasing such sensitivity. TNF neutralizing compounds can be selected [??] from the group consisting of

antibodies, or fragments or portions thereof, peptides, peptido mimetic compounds or organo mimetic compounds that neutralize [neutralizes] TNF activity in vitro, in situ or in vivo, [is considered a TNF neutralizing compound if used according to the present invention.] Screening methods which can be used to determine TNF neutralizing activity of a TNF neutralizing compound can include in vitro or in vivo assays. Such in vitro assays can include a TNF cytotoxicity assay, such as a radioimmuno assay which determines [determine] a decrease in cell death by contact with TNF, such as chimpanzee or human TNF in isolated or recombinant form, wherein the concurrent presence of a TNF neutralizing compound reduces the degree or rate of cell death. The cell death can be determined using ID50 values which represent the concentration of a TNF neutralizing compound which decreases the cell death rate by 50%. For example, MAb's A2 and cA2 are found to have ID50 about 17mg/ml +/- 3mg/ml, such as 14-20 mg/ml, or any range or value therein. Such a TNF cytotoxicity assay is presented in [example] Example II.

Replace the paragraph at page 85, line 31 through page 86, line 7 with the below paragraph marked up by way of bracketing and underlining to show the changes relative to the previous version of the paragraph.

Since the antigen binding domain of cA2 was derived from murine A2, these mAbs would be expected to compete for the same binding site on TNF. Fixed concentrations of chimeric A2 and murine mAb A2 were incubated with increasing concentrations of murine and chimeric A2 competitor, respectively, in a 96-well microtiter plate coated with rhTNF (Dainippon, Osaka, Japan). Alkaline-phosphatase conjugated anti-human immunoglobulin and anti-mouse immunoglobulin second antibodies were used to detect the level of binding of chimeric and murine A2, respectively. Cross-competition for TNF antigen was observed in this solid-phase ELISA format (Figures 9A and 9B [Figure 9]). This finding is consistent with the expected identical epitope specificity of cA2 and murine A2.

Replace the paragraph at page 92, lines 5 through 9 with the below paragraph marked up by way of bracketing and underlining to show the changes relative to the previous version of the paragraph.

Abbreviations: FMOC, 9-fluorenylmethoxycarbonyl; tBu, t-butyl ether; OTB, t-butyl ester; Boc, t-butyloxycarbonyl; Mtr, 4-methoxy-2,3,6-trimethylbenzenesulfonyl; Trt, trityl; OPfp, pentafluorophenylester; ODnbt, oxo-benzotriazole ester [ODhbt, oxo-benzotriazole ster].

Replace the paragraph at page 98, lines 26 through 30 with the below paragraph marked up by way of bracketing and underlining to show the changes relative to the previous version of the paragraph.

Murine and chimeric antibodies, fragments and regions are obtained by construction of chimeric expression vectors encoding the mouse variable region of antibodies obtained in Example XIII [XIV] and human constant regions, as presented in Examples IV-IX above.

Replace the paragraph at page 99, lines 8 through 13 with the below paragraph marked up by way of bracketing and underlining to show the changes relative to the previous version of the paragraph.

Both the murine and chimeric anti-TNF $\alpha$  antibodies of the present invention, as obtained according to Examples XIII and XIV [XIV and XV], are determined to have potent TNF-inhibiting and/or neutralizing activity, as shown for example, in the TNF cytotoxicity assay described above, expressed as the 50% Inhibitory Dose (ID50).

Replace the paragraph at page 99, line 21 through page 100, line 5 with the below paragraph marked up by way of bracketing and underlining to show the changes relative to the previous version of the paragraph.

The ability of both the murine and chimeric anti-TNF $\alpha$  antibodies of the present invention, as obtained according to Examples XIII and XIV [XIV and XV], to inhibit or neutralize human TNF $\alpha$

bioactivity *in vitro* is tested using the bioassay system described above. Cultured cells producing the murine or chimeric anti-TNF $\alpha$  antibodies of the present invention, as obtained according to Examples XIII and XIV [XIV and XV], are incubated with 40 pg/ml natural (Genzyme, Boston, MA) or recombinant (Suntory, Osaka, Japan) human TNF with or without antibody overnight as above, and cell death is measured by vital staining. As expected, both the murine and chimeric anti-TNF $\alpha$  antibodies of the present invention, as obtained according to Examples XIII and XIV [XIV and XV], inhibited or neutralized both natural and rhTNF in a dose-dependent manner in the cytotoxicity assay. Such inhibiting and/or neutralizing potency, at antibody levels below 1  $\mu$ g/ml, can easily be attained in the blood of a subject to whom the antibody is administered. Accordingly, such highly potent inhibiting and/or neutralizing anti-TNF antibodies, in particular the chimeric antibody, are preferred for therapeutic use in TNF $\alpha$ -mediated pathologies or conditions.

Replace the paragraph at page 100, lines 15 through 35 with the below paragraph marked up by way of bracketing and underlining to show the changes relative to the previous version of the paragraph.

The ability of TNF to activate procoagulant and adhesion molecule activities of endothelial cells (EC) is thought to be an important component of pathology pathophysiology. In particular, this can be associated with the vascular damage, disseminated intravascular coagulation, and severe hypotension that is associated with the sepsis syndrome. Therefore, the ability of both the murine and chimeric anti-TNF $\alpha$  antibodies of the present invention, as obtained according to Examples [XIV and XV] XIII and XIV, to block TNF-induced activation of cultured human umbilical vein endothelial cells (HUVEC) is evaluated. TNF stimulation of procoagulant activity is determined by exposing intact cultured HUVEC cells to TNF (with or without antibody) for 4 hours and analyzing a cell lysate in a human plasma clotting assay. The results are expected to show the expected upregulation by TNF of HUVEC procoagulant activity (reflected by a decreased clotting time). Both the murine and chimeric anti-TNF $\alpha$  antibodies of the present invention, as obtained according to

Examples XIII and XIV [XIV and XV], are expected to effectively inhibit or neutralize this TNF activity in a dose-dependent manner.

Replace the paragraph at page 100, line 36 through page 101, line 13 with the below paragraph marked up by way of bracketing and underlining to show the changes relative to the previous version of the paragraph.

In addition to stimulating procoagulant activity, TNF also induces surface expression of endothelial cell adhesion molecules such as ELAM-1 and ICAM-1. The ability of both the murine and chimeric anti-TNF $\alpha$  antibodies of the present invention, as obtained according to Examples XIII and XIV [XIV and XV], are expected to inhibit or neutralize this activity of TNF is measured using an ELAM-1 specific detection radioimmunoassay. Cultured HUVEC are stimulated with 250 ng/ml rhTNF (Dainippon, Osaka, Japan) with or without antibody at 37°C overnight in a 96-well plate format. Surface expression of ELAM-1 is determined by sequential addition of a mouse anti-human ELAM-1 mAb and  $^{125}$ I-labelled rabbit anti-mouse immunoglobulin second antibody directly to culture plates at 4°C.

Replace the paragraph at page 101, lines 20 through 29 with the below paragraph marked up by way of bracketing and underlining to show the changes relative to the previous version of the paragraph.

Finally, TNF is known to stimulate mitogenic activity in cultured fibroblasts. Both the murine and chimeric anti-TNF $\alpha$  antibodies of the present invention, as obtained according to Examples XIII and XIV [XIV and XV], are expected to inhibit or neutralize TNF-induced mitogenesis of human diploid FS-4 fibroblasts cultures, confirming the potent inhibiting and/or neutralizing capability of both the murine and chimeric anti-TNF $\alpha$  antibodies of the present invention, as obtained according to Examples XIII and XIV [XIV and XV] against a broad spectrum of *in vitro* TNF biological activities.

Replace the paragraph at page 102, lines 3 through 22 with the below paragraph marked up by way of bracketing and underlining to show the changes relative to the previous version of the paragraph.

An *in vivo* model wherein lethal doses of human TNF are administered to galactosamine-sensitized mice (Lehmann, V. et al., *infra*) is substantially modified for testing the capability of both the murine and chimeric anti-TNF $\alpha$  antibodies of the present invention, as obtained according to Examples XIII and XIV [XIV and XV] above, to inhibit or neutralize TNF *in vivo*. An i.p. challenge with 5  $\mu$ g (0.25 mg/kg) of rhTNF resulted in 80-90 percent mortality in untreated control animals and in animals treated i.v. 15-30 minutes later with either saline or 2 mg/kg control antibody (a chimeric IgG1 derived from murine 7E3 anti-platelet mAb). In contrast, treatment with both the murine and chimeric anti-TNF $\alpha$  antibodies of the present invention, as obtained according to Examples XIII and XIV [XIV and XV], is expected to reduce mortality to 0-30 percent with 0.4 mg/kg of antibody, and to 0-10 percent with 20 mg/kgs. These expected results indicate that both the murine and chimeric anti-TNF $\alpha$  antibodies of the present invention, as obtained according to Examples XIII and XIV [XIV and XV], are capable of inhibiting and/or neutralizing the biological activity of TNF [*in vivo*] *in vivo* as well as *in vitro*.

Replace the paragraph at page 107, lines 2 through 9 with the below paragraph marked up by way of bracketing and underlining to show the changes relative to the previous version of the paragraph.

Patients were monitored during and for 24 hours after infusions for hemodynamic change, fever or other adverse events. Clinical and laboratory monitoring for possible adverse events was undertaken on each follow-up assessment day. Clinical response parameters were performed at the time-points as specified in the flow charts [chart] presented [present] in Tables 9A and 9B [Table 9]. These evaluations were performed prior to receiving any infusions.

Replace the paragraph at page 125, lines 3 through 28 with the below paragraph marked up by way of bracketing and underlining to show the changes relative to the previous version of the paragraph.

Analysis of improvement in individual patients was made using two separate indices. Firstly, an index of disease activity (IDA) was calculated for each time point according to the method of Mallya and Mace (Mallya et al., *Rheumatol. Rehab.* 20:14-17 (1981), with input variable of morning stiffness, pain score, Ritchie Index, grip strength, ESR and Hgb. The second index calculated was that of Paulus (Paulus et al., *Arthritis Rheum.* 33:477-484 (1990) which uses input variables of morning stiffness, ESR, joint pain/tenderness, joint swelling, patient's and physician's global assessment of disease severity. In order to calculate the presence or otherwise of a response according to this index, two approximations were made to accommodate our data. The 28 swollen joint count used by us (nongraded; validated in Fuchs et al., *Arthritis Rheum.* 32:531-537 (1989)) was used in place of the more extensive graded count used by Paulus, and the patient's and physician's global assessments of response recorded by us were approximated to the global assessments of disease activity used by Paulus *infra*. In addition to determining response according to these published indices, we selected 6 disease activity assessments of interest (morning stiffness, pain score, Ritchie index, swollen joint count, ESR and CRP) and calculated their mean percentage improvement. We have used [figures] Figures 24 and 25 [25 and 26] to give an indication of the degree of improvement seen in responding patients.

Replace the paragraph at page 129, lines 15 through 37 with the below paragraph marked up by way of bracketing and underlining to show the changes relative to the previous version of the paragraph.

*Disease Activity* - The pattern of response for each of the clinical assessments of disease activity and the derived IDA are shown in Table 13. All clinical assessments showed improvement following treatment with cA2, with maximal responses from week 3. Morning stiffness fell from a median of 180 minutes at entry to 5 minutes at week 6 ( $p<0.001$ , adjusted), representing an

improvement of 73%. Similarly, the Ritchie Index improved from 28 to 6 at week 6, ( $p<0.001$ , adjusted, 79% improvement) and the swollen joint count fell from 18 to 5, ( $p<0.001$ , adjusted, 72% improvement). The individual swollen joint counts for all time points are shown in Figure 24 [25]. Grip strength also improved; the median grip strength rose from 77 (left) and 92 (right) mm Hg at entry to 119 (left) and 153 (right) mmHg at week 6 ( $p<0.04$ ,  $p<0.05$ , left and right respectively;  $p>0.05$  after adjustment for multiple comparisons). The IDA showed a fall from a median of 3 at entry to 1.7 at week 6 ( $p<0.001$ , adjusted). Patients were asked to grade their responses to cA2 on a 5 point scale. No patient recorded a response of 'worse' or 'no change' at any point in the trial. ['FaIr'] 'Fair', 'good' and 'excellent' responses were classed as improvements of 1, 2 and 3 grades respectively. At week 6, the study group showed a median of 2 grades of improvement (Table 13).

Replace the paragraph at page 130, lines 6 through 27 with the below paragraph marked up by way of bracketing and underlining to show the changes relative to the previous version of the paragraph.

The changes in the laboratory tests which reflect disease activity are shown in Table 14. The most rapid and impressive changes were seen in serum CRP, which fell from a median of 39.5 mg/liter at entry to 8 mg/liter by week 6 of the trial ( $p<0.001$ , adjusted; normal range <10 mg/liter), representing an improvement of 80%. Of the 19 patients with elevated CRP at entry, 17 showed falls to the normal range at some point during the trial. The improvement in CRP was maintained in most patients for the assessment period (Table 14 and Figure 25 [26]); the exceptions with high values at 4 and 6 weeks tended to be those with the highest starting values (data not shown). The ESR also showed improvement, with a fall from 55 mm/hour at entry to 23 mm/hour at week 6 ( $p<0.03$ ;  $p>0.05$  adjusted; 58% improvement; normal range <10 mm/hour, <15 mm/hour, males and females respectively). SAA levels were elevated in all patients at trial entry, and fell from a median of 245 mg/ml to 58 mg/ml at week 1 ( $p<0.003$ , adjusted; 76% improvement; normal range < 10/mg/ml) and to 80 mg/ml at week 2 ( $p<0.04$ , adjusted). No significant changes were seen in

Hgb, WBC or platelet count at week 6, although the latter did improve at weeks 2 and 3 compared with trial entry (Table 14).

Replace the paragraph at page 139, lines 14 through 35 with the below paragraph marked up by way of bracketing and underlining to show the changes relative to the previous version of the paragraph.

A previously cloned EcoRI fragment containing the cM-T412 heavy chain gene (Goeddel et al., *Cold Spring Harbor Symp. Quant. Biol.* 1986, 51, 597-609) was subcloned into pUC19. This recombinant plasmid was used as a template for two PCR reactions. In one reaction, an oligo corresponding to the "reverse" primer of the pUC plasmids and the 3' oligo 5'-CCTGGATACCTGTGAAAAGA-3' (SEQ ID NO:8) (bold marks half of a StuI site; oligo was phosphorylated prior to the PCR reaction) were used to amplify a fragment containing 3kb of 5' flanking DNA, the promoter, transcription start site and leader peptide coding sequence (including the leader intron). In the second reaction, the 5' oligo 5'CCTGGTACCTTAGTCACCGTCT CCTCA-3' (SEQ ID NO:9) (bold marks half of a StuI site; oligo phosphorylated prior to the PCR reaction) and an oligo corresponding to the "forward" primer of pUC plasmids amplified a fragment encoding eight amino acids of human J sequence Gly Thr Leu Val Thr Val Ser Ser (SEQ ID NO:6) and a splice donor to allow splicing to the human constant region coding sequence provided in another vector. The two PCR fragments were digested with EcoRI and then simultaneously ligated into EcoRI-digested pUC19 to make pHc684 (Figure 27 [28]).

Replace the paragraph at page 139, line 36 through page 140, line 16 with the below paragraph marked up by way of bracketing and underlining to show the changes relative to the previous version of the paragraph.

Because the StuI site formed at the junction of the two PCR fragments was followed by a 'GG' dinucleotide sequence, a *dcm* methylation site was formed preventing StuI from digesting that site when the DNA was grown in HB101 strain of *E coli*. Therefore, the plasmid DNA was

introduced into *dcm*- JM110 *E. coli* cells and reisolated. StuI was then able to cut at the junction but a second StuI site in the 5' flanking DNA was [a] apparent (DNA sequencing showed that StuI site to also be followed by a GG dinucleotide and therefore also methylated). To make the StuI cloning site at the junction be unique, a 790 bp XbaI fragment that included only one of the two StuI sites was subcloned into pUC19 to make the vector pHCH707 (Figure 27 [28A]) which was then grown in JM110 cells. The StuI cloning site formed at the junction of the two PCR fragments second and third nucleotides (i.e., 'CA') of the last codon (Ala) of the signal sequence in order to maintain the appropriate translation reading frame (Figure 27 [28]).

Replace the paragraph at page 140, lines 17 through 33 with the below paragraph marked up by way of bracketing and underlining to show the changes relative to the previous version of the paragraph.

A PCR fragment encoding a protein of interest can then be ligated into the unique StuI site of pHCH707. The insert can include a translation stop codon that would result in expression of a "non-fusion" protein. Alternatively, a fusion protein could be expressed by the absence of a translation stop codon, thus allowing translation to proceed through additional coding sequences positioned downstream of the StuI cloning site. [pHC707 at a unique XbaI site upstream of the IgG1 coding sequences (Figure 29).] Coding sequences in the StuI site of pHCH707 would not be fused directly to the IgG1 coding sequences in pHCH730 but would be separated by an intron sequence that partially originates from pHCH707 and partially from pHCH730. These intron sequences would be deleted in the cell following transcription resulting in an RNA molecule that is translated into a chimeric protein with the protein of interest fused directly to the IgG1 constant domains.

Replace the paragraph at page 140, line 34 through page 141, line 8 with the below paragraph marked up by way of bracketing and underlining to show the changes relative to the previous version of the paragraph.

The plasmid pHC730 was a modified form of an IgG1 expression, pSV2gpt-hCyl vector described previously (Goeddel et al., *Cold Spring Harbor Symp. Quant. Biol.* 1986, 51, 597-609) (Figure 28 [28B]). The modifications were (1) removal of the unique SalI and XbaI sites upstream of the constant region coding sequence, (2) insertion of a SalI linker into the unique BamHI site to allow use of SalI to linearize the plasmid prior to transfections, and (3) ligation into the unique EcoRI site the cloned cM-T412 EcoRI fragment but with the XbaI fragment flanking the V gene deleted (Figure 29 [30]). The resulting expression vector had a unique XbaI site for inserting the XbaI fragments from pHC707.

Replace the paragraph at page 141, lines 10 through 32 with the below paragraph marked up by way of bracketing and underlining to show the changes relative to the previous version of the paragraph.

A previously cloned HindIII fragment containing the cM-T412 light chain gene (Goeddel et al., *Cold Spring Harbor Symp. Quant. Biol.* 1986, 51, 597-609) was subcloned into pUC19 and the resulting plasmid used as template for PCR reactions. In one PCR reaction the "reverse" pUC primer and the 3' oligo 5'-AATAGATATCTCCTCAACACCTGCAA-3' (SEQ ID NO:10) (EcoRV site is in bold) were used to amplify a 2.8 kb fragment containing 5' flanking DNA, the promoter, transcription start site and leader peptide coding sequence (including the leader intron) of the cloned light chain gene. This fragment was then digested with HindIII and EcoRV. In a second PCR reaction, the 5' oligo 5'-ATCGGGACAAAGTTGGAAATA-3' (SEQ ID NO:11) (bold marks half of an EcoRV site) and the "forward" pUC primer were used to amplify a fragment encoding seven amino acids of human J sequence (Gly Thr Lys Leu Glu Ile Lys) and an intron splice donor sequence. This fragment was digested with HindIII and ligated along with the other PCR fragment into pUC cut with HindIII. The resulting plasmid, pLC671 (Figure 29 [30]), has a unique EcoRV cloning site at the junction of the two PCR fragments with the EcoRV site positioned such that the first three nucleotides of the EcoRV site encoded the first amino acid of the mature protein (Asp).

Replace the paragraph at page 141, line 33 through page 142, line 25 with the below paragraph marked up by way of bracketing and underlining to show the changes relative to the previous version of the paragraph.

The pLC671 HindIII insert was designed to be positioned upstream of coding sequences for the human kappa light chain constant region present in a previously described expression vector, pSV2gpt-hCk (Figure 30 [31]). However, pSV2gpt-hCk contained an EcoRV site in its *gpt* gene. Because it was desired that the EcoRV site in the pLC671 HindIII fragment be a unique cloning site after transferring the fragment into pSV2gpt-hCk, the EcoRV site in pSV2gpt-hCk was first destroyed by PCR mutagenesis. Advantage was taken of the uniqueness of this EcoRV site in pSV2gpt-hCk and a Kpn1 site 260 bp upstream of the EcoRV site. Therefore, the 260 bp Kpn1-EcoRV fragment was removed from pSV2gpt-hCk and replaced with a PCR fragment that has identical DNA sequence to the 260 bp fragment except for a single nucleotide change that destroys the EcoRV site. The nucleotide change that was chosen was a T to a C in the third position of the EcoRV recognition sequence (i.e., GATATC changed to GACATC). Because the translation reading frame is such that GAT is a codon and because both GAT and GAG codons encode an Asp residue, the nucleotide change does not change the amino acid ended at that position. Specifically, pSV2gpt-hCk was used as template in a PCR reaction using the 5' oligo 5'GGCGGTCT GGTACCGG-3' (SEQ ID NO:12) (Kpn1 site is in bold) and the 3' oligo 5'-GTCAACAA**C**ATAGTCATCA-3' (SEQ ID NO: 13) (bold marks the complement of the ASP codon). The 260 bp PCR fragment was treated with the Klenow fragment of DNA polymerase to fill-in the DNA ends completely and then digested with Kpn1. The fragment was ligated into pSV2gpt-hCk that had its Kpn1-EcoRV fragment removed to make pLC327 (Figure 30 [31]).

Replace the paragraph at page 142, lines 26 through 35 with the below paragraph marked up by way of bracketing and underlining to show the changes relative to the previous version of the paragraph.

The HindIII fragment of pLC671 was cloned into the unique HindIII site of pLC327 to make the light chain expression vector, pLC690 (Figure 30 [31]). This plasmid can be introduced into cells without further modifications to encode a truncated human kappa light chain, JCk, that contains the first two amino acids of the cM-T412 light chain gene, seven amino acids of human J sequences, and the light chain constant region. Alternatively, coding sequence of interest can be introduced into the unique EcoRV site of pLC690 to make a light chain fusion protein.

Replace the paragraph at page 145, lines 10 through 26 with the below paragraph marked up by way of bracketing and underlining to show the changes relative to the previous version of the paragraph.

After one or two rounds of subcloning, spent cell supernatant from the various cell lines were yielding 20 µg/ml (for p55-sf2) of fusion protein. The proteins were purified from the spent supernatant by protein A column chromatography and analyzed by SDS-PAGE with or without a reducing agent [(Figure 32)]. Each fusion protein was clearly dimeric in that their  $M_r$  estimates from their migration through a non-reducing gel was approximately double the estimated  $M_r$  from a reducing gel. However, two bands were seen for p55-sf2 [(Figure 32, lane 1)] and p55-df2. Two lines of evidence indicated that, in each case, the lower bands did not include a light chain while the upper bands did include a light chain. First, when p55-sf2 containing both bands were passed over an anti-kappa column, the upper band bound to the column (lane 3) while the lower band passed through the column. Second, Western blots have shown that only the upper bands were reactive with anti-kappa antibodies.

Replace the paragraph at page 146, lines 1 through 14 with the below paragraph marked up by way of bracketing and underlining to show the changes relative to the previous version of the paragraph.

The ability of the various fusion proteins to bind and neutralize human TNF $\alpha$  or TNF $\beta$  was tested in a TNF-mediated cell killing assay. Overnight incubation of the murine fibrosarcoma cell

line, WEHI 164 (Espevik et al., *J. Immunol. Methods* 1986, 95, 99-105), with 20 pM (1 ng/ml) TNF $\alpha$  results in essentially complete death of the culture. When the fusion proteins were pre-incubated with TNF $\alpha$  (Figure 31A [33A]) or TNF $\beta$  (Figure 31B [33B] and Table 1 above) and the mixture added to cells, each fusion protein demonstrated dose-dependent protection of the cells from TNF cytotoxicity. Comparison of the viability of control cells not exposed to TNF to cells incubated in both TNF and fusion protein showed that the protection was essentially complete at higher concentrations of fusion protein.

Replace the paragraph at page 146, lines 15 through 29 with the below paragraph marked up by way of bracketing and underlining to show the changes relative to the previous version of the paragraph.

Tetravalent p55-df2 showed the greatest affinity for TNF $\alpha$  requiring a concentration of only 55 pM to confer 50% inhibition of 39 pM (2 ng/ml) TNF $\alpha$  (Figure 31A [33A] and Table 1). Bivalent p55-sf2 and p75P-sf2 were nearly as efficient, requiring concentrations of 70 pM to half-inhibit TNF $\alpha$ . Approximately two times as much p75-sf2 was required to confer 50% inhibition compared to p55-sf2 at the TNF concentration that was used. The monomeric, non-fusion form of p55 was much less efficient at inhibiting TNF $\alpha$  requiring a 900-fold molar excess over TNF $\alpha$  to inhibit cytotoxicity by 50%. This much-reduced inhibition was also observed with a monomeric, Fab-like p55 fusion protein that was required at a 2000-fold molar excess over TNF $\alpha$  to get 50% inhibition. The order of decreasing inhibitory activity was therefore p55-df2 > p55-sf2 = p75P-sf2 > p75-sf2 >> monomeric p55.

Replace the paragraph at page 147, lines 19 through 21 with the below paragraph marked up by way of bracketing and underlining to show the changes relative to the previous version of the paragraph.

Similar to p55-sf2, [as presented in Figure 32,] two bands were seen for p75-sf2 [(Figure 32A, lane 7)] and p75P-sf2 [(Figure 32B, lane 8)].

Replace the paragraph at page 147, lines 22 through 29 with the below paragraph marked up by way of bracketing and underlining to show the changes relative to the previous version of the paragraph.

Surprisingly, the order of decreasing inhibitory activity was different for TNF $\beta$ , as presented in Figure 32 [34]. p75P-sf2 was most efficient at inhibition requiring a concentration of 31 pM to half-inhibit human TNF $\beta$  at 2 pM. Compared to p75P-sf2, three times as much p75-sf2 and three times as much p55-sf2 were necessary to obtain the same degree of inhibition. The order of decreasing inhibitory activity was therefore p75P-sf2 > p75-sf2 = p55-sf2.

Replace the paragraph at page 147, line 31 through page 148, line 10 with the below paragraph marked up by way of bracketing and underlining to show the changes relative to the previous version of the paragraph.

A comparison was made of the binding affinity of various fusion proteins and TNF $\alpha$  by saturation binding (Figure 33A [35A]) and Scatchard analysis (Figure 33B [35B]). A microtiter plate was coated with excess goat anti-Fc polyclonal antibody and incubated with 10 ng/ml of fusion protein in TBST buffer (10 mM Tris-HCl [HCl], pH 7.8, 150 NaCl [NaCl], 0.05% Tween-20) for 1 hour. Varying amounts of  $^{125}$ I labeled TNF $\alpha$  (specific activity - 34.8  $\mu$ Ci/ $\mu$ g) was then incubated with the captured fusion protein in PBS (10 mM Na Phosphate, pH 7.0, 150 mM NaCl) with 1% bovine serum albumin for 2 hours. Unbound TNF $\alpha$  was washed away with four washes in PBS and the cpm bound was quantitated using a y-counter. All samples were analyzed in triplicate. The slope of the lines in (B) represent the affinity constant,  $K_a$ . The dissociation constant ( $K_d$ ) values (see Table 1) were derived using the equation  $K_d = 1/K$ .